A free energy study of carbon clusters on Ir(111): Precursors to graphene growth

H. Tetlow,[1] I. J. Ford,[2] and L. Kantorovich[2]

[1)] *Department of Physics, King's College London, The Strand, London, WC2R 2LS, United Kingdom*

[2)] *Department of Physics and Astronomy and London Centre for Nanotechnology, University College London, Gower Street, London, WC1E 6BT, United Kingdom*

It is widely accepted that the nucleation of graphene on transition metals is related to the formation of carbon clusters of various sizes and shapes on the surface. Assuming a low concentration of carbon atoms on a crystal surface, we derive a thermodynamic expression for the grand potential of the cluster of N carbon atoms, relative to a single carbon atom on the surface (the cluster work of formation). This is derived taking into account both the energetic and entropic contributions, including structural and rotational components, and is explicitly dependent on the temperature. Then, using *ab initio* density functional theory, we calculate the work of formation of carbon clusters C_N on the Ir(111) surface as a function of temperature considering clusters with up to $N = 16$ C atoms. We consider five types of clusters (chains, rings, arches, top-hollow and domes), and find, in agreement with previous zero temperature studies, that at elevated temperatures the structure most favoured depends on N, with chains and arches being the most likely at $N < 10$ and the hexagonal domes becoming the most favourable at all temperatures for $N > 10$. Our calculations reveal the work of formation to have a much more complex character as a function of the cluster size than one would expect from classical nucleation theory: for typical conditions the work of formation displays not one, but two nucleation barriers, at around $N = 4 - 5$ and $N = 9 - 11$. This suggests, in agreement with existing LEEM data, that five atom carbon clusters, along with C monomers, must play a pivotal role in the nucleation and growth of graphene sheets, whereby the formation of large clusters is achieved from the coalescence of smaller clusters (Smoluchowski ripening). Although the main emphasis of our study is on thermodynamic aspects of nucleation, the pivotal role of kinetics of transitions between different cluster types during the nucleation process is also discussed for a few cases as illustrative examples.

I. INTRODUCTION

One of the main challenges facing the widespread commercial exploitation of graphene is our limited ability to produce it in large quantities with high enough quality[1]. The methods currently used to grow graphene usually involve depositing a hydrocarbon source material C_NH_M onto a transition metal surface, followed by heating to high temperatures to facilitate dehydrogenation reactions with subsequent evaporation of hydrogen from the surface. It is now clear that during the growth process graphene islands must originate from smaller carbon clusters[2–4], which in turn must nucleate on the surface from a carbon source. Recent work has shown that ethylene (which is often used for graphene growth) deposited on the Ir(111) surface at room temperature with subsequent heating to higher temperatures, will decompose completely into carbon monomers[5]. These act as building blocks for the carbon clusters that go on to form graphene islands. In order to develop a clear understanding of graphene nucleation, the required initial stage of graphene growth, it is necessary to investigate the thermodynamics of the formation of carbon clusters on transition metal surfaces. This should take into account the energetic as well as the entropic contributions to the free energy of cluster formation relevant to the high temperatures where the growth is observed experimentally. Here we present a study of this kind based on *ab initio* density functional theory (DFT) that for the first time, to the best of our knowledge, explicitly takes into account temperature dependent, entropic contributions to the work of formation of clusters.

In temperature programmed growth (TPG) experiments[1] the nature of intermediate carbon clusters has been identified for a variety of metal growth surfaces. On the Rh(111), Ru(0001) and Ir(111) surfaces dome-like clusters containing 13 or more C atoms organised in hexagonal rings have been observed at temperatures ranging from 770 to 900 K, prior to the initiation of graphene growth[3,4,6,7]. DFT calculations for the Ir(111) surface have shown that these dome-like clusters are

stabilised by the strong attachment to the surface of the C atoms around their perimeter[6]. Experiments using LEEM analysis have also determined the dependence of the graphene growth rate on the concentration of C monomers[8]. In this case the dependence of the growth rate on the fifth power of monomer concentration suggests Smoluchowski type aggregation[9], where the growth of graphene on Ir(111) involves the coalescence of five atom carbon clusters to form graphene nuclei followed by their addition to existing islands. Therefore these clusters are expected to be stable on the surface, and they must play an essential role in nucleating graphene sheets.

According to classical nucleation theory[1,10,11], the rate of nucleation is proportional to the rate of formation of clusters with a particular (critical) number N^* of carbon atoms. Structures of such critical size are equally likely to grow further (by accepting more atoms) or to decrease in size (by expelling atoms). The value of N^* is determined by the *free energy of cluster formation,* or nucleation work, a function of cluster size N that has a maximum at the critical size. Clusters with $N > N^*$ are more likely to grow rather than decay, and the reverse applies for $N < N^*$. Hence, calculating the nucleation work for various cluster sizes and shapes at various temperatures is absolutely fundamental for developing an understanding of their propensity to grow or decay.

Previously, the stability of small carbon clusters with different structures with N up to 24, on various surfaces, has been studied using DFT calculations[1,12–17]. Typically in these studies the formation energy (or a variant of this quantity) for each cluster was calculated at zero temperature, and this was used to determine the stability of the clusters. For clusters on the Cu(111) surface it was found[14] that linear (arching) clusters have a lower formation energy and are more stable than compact clusters with $N = 1 - 13$. This was also the case on the Ir(111) surface[12,13] for $N = 1 - 10$. On the Rh(433) step edge it was found that linear clusters are more stable for $N < 10$, but above this sp^2 networks become more

stable[15]. However for Ir step edges (Ir(322) and Ir(223) surfaces) the formation energies for all cluster sizes are reduced, and in some cases the compact structures are more stable than the linear ones[12]. This suggests that clusters may prefer to nucleate at step edges rather than on terraces[15,18]. Nevertheless, the actual location of nucleation has been shown to depend on experimental conditions: depositing the hydrocarbon source at low temperatures, and then heating, results in growth that begins on terraces, to be compared with depositing at high temperatures which initiates the growth at step edges[2]. This is perhaps due to the increased mobility of species at higher temperatures. For larger clusters ranging from 16 to 26 C atoms the formation energies of compact clusters on the Ni(111), Cu(111), Ru(0001), and Rh(111) surfaces were calculated in Ref.[7,19]. It was found that a particular compact cluster containing $N = 21$ atoms was the most stable. These clusters were also observed experimentally on Ru(0001) and Rh(111)[3,4]. Overall, the results of these DFT calculations suggest that smaller clusters are more stable with a linear or arching structure, and as they grow, compact structures become more favourable.

In addition in some cases[7,15,20] the Helmholtz free energy for clusters has been calculated and used to determine the critical cluster size for a range of values of the difference in chemical potential of the surface adsorbed carbon monomer phase with respect to the bulk film. For Ni(111) the critical cluster size was found[20] to be $N = 12$ on terraces and $N = 10$ on step edges with the chemical potential difference between 0.3 and 0.8 eV, suggesting that nucleation will be preferred at step edges rather than terraces. On Rh(433) the critical cluster size was $N = 10$ over a similar range of the chemical potential difference[15]. However in all these studies the free energy was calculated at zero temperature (with the only exception being Ref.[7] where the free energy of a single vibrational mode was added) and any entropic contributions were neglected.

In order to develop an understanding of the kinetics of cluster formation, DFT-

based Nudged Elastic Band (NEB) calculations to determine energy barriers associated with cluster diffusion and growth have been performed in a few cases[21,22]. For the Ni(111) surface the diffusion barriers of small clusters with $N = 1-4$ were calculated[21]. From this it was determined that "star" clusters may be the nuclei of growth, since they are immobile compared to other cluster types such as chains which were found to be highly mobile. The transition barrier from a chain to a star-like cluster was found to be significant on Ni(111) (1.55 eV). The transition between a C_6 compact ring and a linear chain on Cu(111) was investigated in Ref.[14], and the energy barrier for this was found to be 0.66 eV.

The nucleation of graphene has also been considered with kinetics simulations. Molecular dynamics[16,17,22–26] and Monte Carlo[27,28] simulations (see also reviews[18,29–31]) have been performed at high temperatures in order to determine the nucleation process during the growth of graphene and carbon nanotubes (CNTs). For instance, according to one theory[18,30], on Cu(111), Ni(111) and Fe(111) surfaces, as well as on nanoclusters, graphene networks are formed by a distinct mechanism. First C dimers are formed from monomers. These then grow to form small chain-like clusters on the surface. As these grow and diffuse on the surface they connect and intersect to form so-called "Y junctions". Finally, sp^2 type clusters and graphene networks are formed. These simulations of the growth kinetics suggest that nucleation begins with the formation of linear chain structures which then connect to form larger compact sp^2 networks. In spite of the fact that these methods enable one to perform long-time simulations of the early stages of graphene nucleation and growth, their obvious disadvantage is that they are deemed to be based on empirical techniques (classical force fields or tight-binding methods) and hence their accuracy may not be completely satisfactory. On the other hand, a fully *ab initio* DFT treatment of nucleation based on molecular dynamics simulations would be too computationally expensive even for modern supercomputers. An alternative lies in performing a fully *thermodynamic* consideration of graphene

nucleation, based on the ideas of classical nucleation theory, though incorporating microstructural information rather than any continuum approximations. This has a benefit of approaching the problem with state-of-the-art *ab initio* DFT methods without the need to run expensive molecular dynamics simulations, and hence providing valuable insights into the free energetics and statistical behaviour of carbon clusters at a wide range of temperatures characteristic of those used in actual experiments.

Therefore, a thermodynamic study of graphene nucleation based on *ab initio* DFT calculations is the main goal of this paper. We determine the stability of different sized clusters as a function of the growth temperature. So far, in DFT studies of cluster stability, only the zero temperature formation energies have been considered. However, it is well known that graphene growth is initiated only at rather high temperatures, so that calculating zero temperature formation energies may be highly misleading. To determine an appropriate thermodynamic work of formation of each cluster valid at sufficiently high temperatures, the free energy with structural entropic terms must be considered. More precisely, we need to determine the change in grand potential $\Delta\phi$ associated with the formation of the cluster[32]. In addition, to illustrate the role of kinetics in reconstructing the clusters from one type to another, we go beyond thermodynamics and consider some typical transformations between cluster types using DFT based NEB calculations. From this we are able to draw conclusions about the formation of different cluster types during graphene nucleation.

In this paper we shall first derive an expression for $\Delta\phi$ for a carbon cluster of N atoms adsorbed on a crystal surface. The expression includes the structural and vibrational contributions to the energy and entropy. Then, using DFT calculations, we determine this quantity for carbon clusters C_N adsorbed on the Ir(111) terrace, with N taking values up to 16. For each N, clusters with different shapes have been considered (over 50 altogether): it should be noted that only a few of the

linear and compact structures considered here have been studied previously.

The format of the paper is as follows. We start by deriving an expression for the thermodynamic work of on-surface formation of a cluster of N carbon atoms from monomers on the surface. The result depends on the cluster cohesive energy, the vibrational energy and entropy, and contributions from rotational degrees of freedom; the final expression also contains the extent of monomer surface coverage. By using DFT-based calculations we determine these values for each cluster in order to calculate the total work of formation and its dependence on temperature. From this we re-examine the stability of different cluster structures and determine the structure of $\Delta\phi$ as a function of N which enables us to discuss the critical cluster size N^* that is associated with the nucleation barrier[1,10,11] and sets the minimum size at which stable clusters form. This consideration allows us to predict the nucleation mechanism at different temperatures without explicitly simulating the kinetics. We then discuss possible cluster growth mechanisms based on our NEB simulations of the transformation between different cluster types. The paper ends with a brief discussion and conclusions.

II. THEORY

A. Derivation of cluster formation energy

Nucleation theory provides the rate of formation, per unit area of substrate, of a cluster of N atoms from a gas of monomers[32],

$$J = n_1 Z \beta_{N^*} \exp(-\Delta\phi(N)/k_B T) \; . \tag{1}$$

Here n_1 is the monomer concentration on the surface, Z is the Zeldovich factor, k_B is Boltzmann's constant and β_{N^*} is the rate of monomer attachment to a critical cluster of size N^*. $\phi(N)$ denotes the grand potential for the N atom cluster, and $\Delta\phi(N) = \phi(N) - \phi(1)$ in the exponent in Eq. (1) corresponds to the grand

potential of the cluster relative to a single adsorbed carbon atom. The dependence of this quantity on N gives the barrier for nucleation and the corresponding critical cluster size N^*.

For an N atom cluster the grand potential $\phi(N)$ can be expressed in terms of the cluster free energy $F(N)$ and the chemical potential of the monomer gas μ in the following way:

$$\phi(N) = F(N) - N\mu \; . \tag{2}$$

The Helmholtz free energy is related in the usual way to the cluster partition function $Z(N)$, namely $F(N) = -k_B T \, \ln Z(N)$, and for solid-like clusters $Z(N)$ can take the form

$$Z(N) = N_{\rm sites} N_{\rm rot} Z^{\rm vib}(N) {\rm e}^{-U(N)/k_B T} \; . \tag{3}$$

This expression contains entropic multiplicity terms related to the number of locations the cluster can occupy on a finite substrate of $N_{\rm sites}$ sites, and the number of rotational variants, $N_{\rm rot}$, a cluster can take at the same lattice site (which will depend on its shape). It is assumed that there is a sufficiently low concentration of clusters on the surface so that interactions between different clusters can be neglected. The exponential Boltzmann factor contains the energy $U(N)$ of a single cluster on the surface at zero temperature, while the last factor, $Z^{\rm vib}(N)$, accommodates the appropriate vibrational contribution for the surface and adsorbed cluster. The energy may be written $U(N) = U_0 + \Delta U(N)$, where U_0 is the energy of the isolated surface and $\Delta U(N)$ represents the energy of an isolated cluster plus the interaction energy of the cluster with the surface as well as the corresponding relaxation energy of both the surface and the cluster.

Hence, the free energy of the cluster on the surface is

$$F(N) = -k_B T \, \ln \left(N_{\rm sites} N_{\rm rot} \right) + U_0 + \Delta U(N) + F^{\rm vib}(N) \; , \tag{4}$$

where $F^{\rm vib}(N) = -k_B T \, \ln Z^{\rm vib}(N)$ is the vibrational contribution to the free energy. To calculate the latter, we note that the combined vibrational density of states (DOS) of the cluster and surface system $D(\omega)$ can be expressed as

$$D(\omega) = D_0(\omega) + \Delta D_N(\omega) \; , \tag{5}$$

where

$$D_0(\omega) = \sum_{\lambda \in S_0} \delta \left(\omega - \omega_\lambda \right) \tag{6}$$

is the DOS of the isolated surface and

$$\Delta D_N(\omega) = \sum_{\lambda \in S + {\rm C}_N} \delta \left(\omega - \omega_\lambda \right) - \sum_{\lambda \in S_0} \delta \left(\omega - \omega_\lambda \right) \tag{7}$$

is the change in the total DOS due to the adsorbed ${\rm C}_N$ cluster. The first term in $\Delta D_N(\omega)$ contains the sum over all vibrational modes of the cluster and surface system ${\rm C}_N + S$, while only the modes of the isolated surface, S_0, are accounted for in the second. Hence,

$$F^{\rm vib}(N) = F_0^{\rm vib} + \Delta F^{\rm vib} \; , \tag{8}$$

where $F_0^{\rm vib}$ is the vibrational free energy of the isolated surface, and

$$\begin{aligned} \Delta F^{\rm vib}(N) &= -k_B T \int \Delta D_N(\omega) \ln Z^{\rm vib}(\omega) d\omega = \int \Delta D_N(\omega) F^{\rm vib}(\omega) d\omega \\ &= \sum_{\lambda \in S + C_N} F^{\rm vib} \left(\omega_\lambda \right) - \sum_{\lambda \in S_0} F^{\rm vib} \left(\omega_\lambda \right) \end{aligned} \tag{9}$$

is the free energy change due to the adsorbed cluster. Here

$$F^{\rm vib}(\omega) = -k_B T \, \ln Z^{\rm vib}(\omega) = \frac{1}{2} \hbar \omega + k_B T \, \ln \left(1 - {\rm e}^{-\hbar \omega / k_B T} \right) \tag{10}$$

is the free energy of a single harmonic oscillator of frequency ω and the associated partition function is $Z^{\rm vib}(\omega)$.

Combining all the expressions given above, we obtain for the grand potential of the N atom cluster ${\rm C}_N$ on the surface an expression:

$$\phi(N) = -k_B T \, \ln \left(N_{\rm sites} N_{\rm rot} \right) + \left(U_0 + F_0^{\rm vib} \right) + \Delta U(N) + \Delta F^{\rm vib}(N) - \mu N \; . \tag{11}$$

The quantity $\phi(1)$ needed to calculate the difference $\Delta\phi(N) = \phi(N) - \phi(1)$ is obtained from the above expression by setting $N = 1$. Note that $U_0 + F_0^{\rm vib}$ term is cancelled out in the difference.

Next, we have to calculate the chemical potential μ of the monomer gas of carbon atoms on the surface at temperature T. Note that carbon atoms preferentially occupy hcp lattice sites[5] and hence one C atom can be assigned to a single lattice site. In this case we have a distribution of N carbon atoms on $N_{\rm sites}$ sites on the surface giving $N_{\rm sites}!/\left[N!\,(N_{\rm sites}-N)!\right]$ possibilities. Assuming that $N \ll N_{\rm sites}$ (the limit of small concentration), we may neglect the interaction between carbon atoms. Then the total energy of the system of monomers $U^{\rm C}(N) = U_0 + N\Delta U(1)$ is simply additive, where $\Delta U(1)$ is the energy of a single adsorbed C atom on the surface calculated relative to the energy U_0 of the isolated surface. Similarly, the vibrational free energy $F_{\rm C}^{\rm vib} = F_0^{\rm vib} + N\Delta F^{\rm vib}(1)$ is also additive, with $\Delta F^{\rm vib}(1)$ being the change to the free energy of the surface and a single C atom upon its adsorption. It is given by the expression analogous to Eq. (9). Therefore, repeating the arguments employed in deriving Eq. (11), we can write the following expression for the free energy of N mutually non-interacting carbon atoms on the surface (the monomer gas),

$$F_m(N) = -k_B T \ln \frac{N_{\rm sites}!}{N!(N_{\rm sites}-N)!} + \left(U_0 + F_0^{\rm vib}\right) + N\Delta U(1) + N\Delta F^{\rm vib}(1)\ . \quad (12)$$

The required chemical potential of the monomer gas is then obtained from its definition as

$$\mu = \left(\frac{\partial F_m}{\partial N}\right)_T = \Delta U(1) + \Delta F^{\rm vib}(1) - k_B T\, \ln \frac{1-\theta}{\theta}\ , \quad (13)$$

where $\theta = N/N_{\rm sites}$ is the monomer coverage and Stirling's approximation was used when differentiating the first term in the free energy.

Combining the obtained expression (11) for the grand potential and that for the chemical potential of the free monomer gas of carbon atoms, Eq. (13), the required

expression for the grand potential difference (denoted the *work of formation* hereafter) is finally obtained:

$$\Delta\phi(N) = [\Delta U(N) - N\Delta U(1)] + \left[\Delta F^{\mathrm{vib}}(N) - N\Delta F^{\mathrm{vib}}(1)\right] - k_B T \ln N_{\mathrm{rot}} + (N-1)k_B T \ln \frac{1-\theta}{\theta} \,. \tag{14}$$

Note that $\Delta\phi(N)$ depends not only on N, but also on the monomer coverage θ and the temperature T. The latter dependence comes from the vibrational free energies and the two final terms which depend linearly on T and originate from the configurational entropy contribution.

B. Calculation methods

In order to evaluate the work of formation via Eq. (14) for a cluster of size N, we need to calculate the zero temperature energy differences $\Delta U(N)$ and $\Delta U(1)$, as well as the vibrational free energy terms $\Delta F^{\mathrm{vib}}(N)$ and $\Delta F^{\mathrm{vib}}(1)$ using DFT. Firstly, the geometry of each cluster was optimised on the Ir(111) surface using the CP2K code[33]. The surface consists of a 8×8 cell with four layers, the bottom two of which are fixed to the Ir bulk geometry while the upper layers are allowed to relax. The vacuum gap is chosen to be greater than 15 Å. For the relaxations the generalised gradient approximation (GGA) with the PBE exchange-correlation functional[34] is used along with Goedecker-Teter-Hutter (GTH) pseudopotentials[35] and the optimised m-DZVP basis set[36] with a plane wave cutoff energy of 300 Ry. This cutoff is sufficient for our purposes as the adsorption energies were found converged to 0.0004 eV with respect to the bigger cutoff of 450 Ry. The geometries are relaxed until the force on the atoms is less than 0.038 eV/Å. The DFT-D3 method was used for van der Waals forces[37]. The Nudged Elastic Band (NEB) calculations were used to calculate the energy barriers for the transformation between several cluster types; these calculations were performed using the climbing-image NEB method CI-NEB[38–41]. Nine images were used for each NEB.

Multiple cluster geometries were considered for each value of N, some of which are based on those found in previous calculations by other authors[6,12,13]. In order to find further low energy structures we concentrated on certain types of structures which are low in energy and extended these for different N by adding extra C atoms to their periphery. To compare zero temperature energies of various clusters we also calculated the zero temperature formation energy defined as

$$E_F(N)_{T=0} = \Delta U(N) - N\Delta U(1) \; . \tag{15}$$

This energy is obtained from the work of formation, Eq. (14), by setting $T = 0$ and neglecting the zero-point vibration energies.

To calculate $\Delta F^{\rm vib}(N)$, vibrational frequencies of the cluster C_N adsorbed on the surface as well as of those of the isolated surface are required and to calculate $\Delta F^{\rm vib}(1)$ we also need the vibrational frequencies of a single carbon atom on the surface. In each case the required vibrational frequencies are found using a vibrational analysis routine within the CP2K code[33].

III. RESULTS

A. Zero temperature formation energy

Clusters containing up to $N = 16$ carbon atoms have been studied. The clusters are distinguished by the number of carbon atoms involved (C, C_2, etc.), and their type: arches, rings, top-hollow (TH) clusters, chains and domes. Altogether, 56 clusters were considered. The relaxed geometries of the most energetically stable clusters of each type are shown in Fig. 1. All other cluster structures are presented in the supplementary material. The zero temperature formation energies of the clusters, as given in Eq. (15), are shown in Fig. 2. For carbon monomers the lowest energy position is the hcp surface site. The C_2 and C_3 cluster geometries are simple chains of atoms, where each atom rests in a hollow site, centred between three Ir

atoms. For larger clusters multiple geometries become possible for the same value of N. We consider stable chain structures with N up to 6 where the atoms are all located in hollow sites at similar distances from the surface. Arching clusters can also be formed where the linear chain of atoms bends so that, in many cases, only the atoms at the ends of the arch interact strongly with the substrate. It is also possible to form stable compact clusters by arranging C atoms in alternating top (on top of an Ir atom) and hollow sites, with the outer atoms in hollow sites. These are referred to as top-hollow (TH) clusters. These clusters are slightly dome-like, where the inner atoms, which are positioned slightly away from the surface, interact less strongly with it than the outer (peripheral) atoms which are positioned closer to the surface. A different type of a compact cluster can also be formed by arranging C atoms in a closed ring around Ir surface atoms. Rings containing between 4 and 8 carbon atoms have been considered. In addition, for 10-16 C atoms dome-like clusters (domes) formed of pentagonal or hexagonal rings, similar to those proposed in the literature (see, e.g.[4,6]), were also considered and found to be highly stable. TH clusters may contain hexagons inside them; however, in contrast to the dome clusters, they have a large number of low-coordinated C atoms at their periphery.

We find that the most stable type of cluster at zero temperature varies depending on the value of N. For $N = 4$ the TH cluster (blue curve in Fig. 2) is the most stable, while the arching clusters are more stable for N between 5 and 8 and the chain clusters become less stable. For C_6 and C_9 the hexagonal ring cluster (green) and the TH cluster (blue), respectively, have formation energies similar to the corresponding arching clusters, owing to their symmetry on the surface. Above $N = 10$, TH clusters are more stable than linear arching clusters. The domes (purple curve) tend to have the lowest formation energy amongst all types of clusters starting from $N = 11$.

It is most likely that clusters grow in size by the attachment of C atoms to them.

This procedure will result in some rearrangement of the cluster on the surface and relaxation, but it is unlikely that there will be a significant reconstruction of the inner cluster structure. Therefore, it is expected that the cluster type will be preserved, at least for some time after attachment. This may lead to formation of clusters which are less energetically favourable than clusters of another type of the same size N. Converting between two cluster types would require a complete or significant reconstruction of the cluster which is likely to be associated with a considerable energy barrier. The values of these barriers are closely related to the lifetime of less favourable clusters. The highlighted atoms in the cluster structures in Fig. 1 illustrate how the larger stable clusters may be formed by the addition of atoms to smaller stable clusters. For the chain, ring and arch structures one atom is simply added at a time. For chains, adding atoms makes the clusters generally less stable. The same is true for arches and rings starting from $N = 8$ and $N = 6$, respectively. The general trend for TH structures is that they become more stable when the cluster increases beyond a size of $N = 8$; however, this dependence on N is not monotonic. The addition of two or three C atoms may be required simultaneously in order to jump to the most stable structures (C_7, C_{12}, C_{15}). In some cases a considerable rearrangement of peripheral carbon atoms is required to happen after adding an atom: this is seen in the sequences $C_9 \rightarrow C_{10} \rightarrow C_{11}$ and $C_{14} \rightarrow C_{15} \rightarrow C_{16}$ for TH clusters, see Fig. 1.

B. Temperature dependent work of formation

So far our discussion has been focused on the formation energy in the zero temperature limit, as given by Eq. (15). For conditions of graphene growth the actual temperature reaches over 1000 K and therefore it is important to include temperature dependent terms when analysing cluster stability. This requires calculating the work of formation using Eq. (11) in each case, involving the calculation of

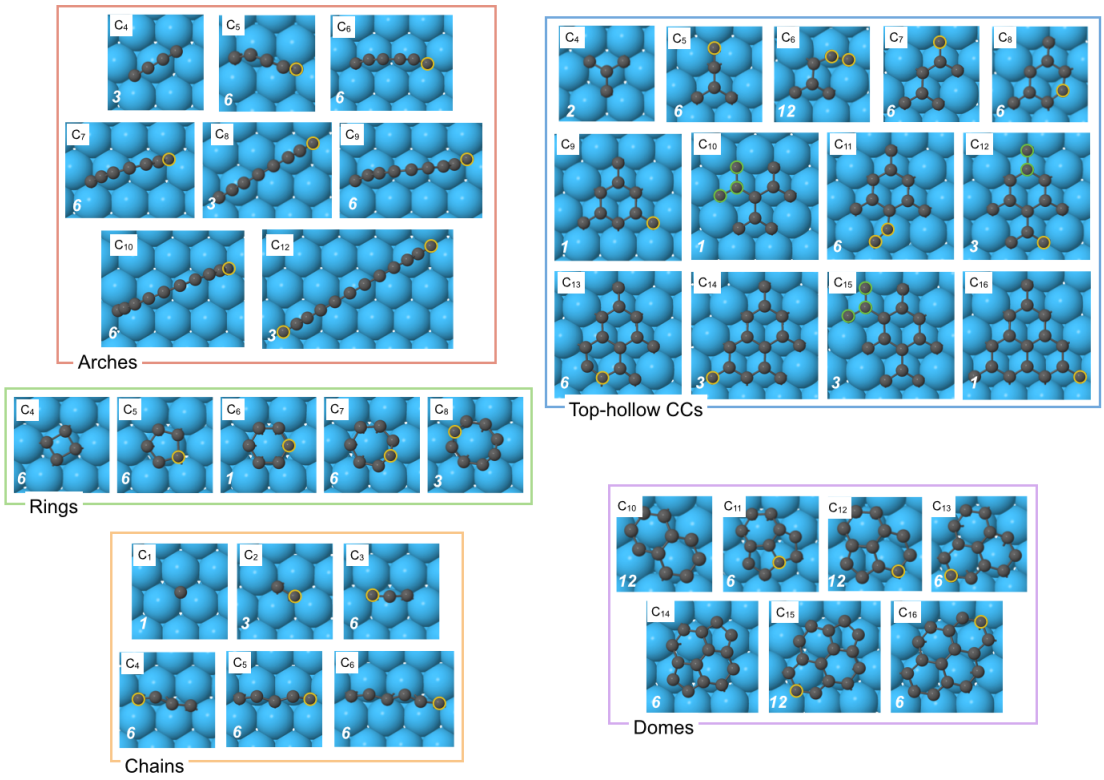

FIG. 1. Top view images showing the relaxed (zero temperature) geometries of various types of the most stable carbon clusters on the Ir(111) surface. The number of carbon atoms in each cluster is shown in the upper-left corner of each figure, with the rotational multiplicities $N_{\rm rot}$ in the lower-left corner. The clusters shown are distributed over five types which are boxed together: arches, rings, top-hollow, chains and domes. Highlighted yellow atoms indicate how the given clusters could be formed by adding a C atom from the previous one in the same box (see text). The highlighted green atoms show the additional atoms required to jump between the most stable top-hollow cluster structures (C_7, C_{10}, C_{12}, C_{15}).

vibrational frequencies for the perfect surface, for the surface with a single carbon atom adsorbed on it, as well as for every carbon cluster on the surface we have considered. Additionally, rotational multiplicities, $N_{\rm rot}$, need to be established for

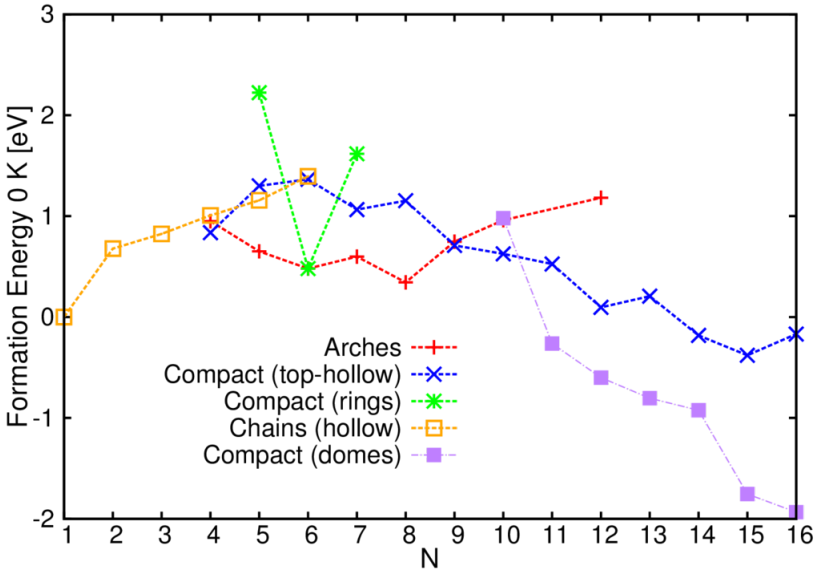

FIG. 2. DFT calculated formation energies (at $T = 0$) of all clusters shown relative to the energy of a single carbon atom on the surface.

each cluster studied. These are defined entirely by the cluster's symmetry and are given in Fig. 1.

In Fig. 3 the work of formation of each cluster studied is shown for a number of temperatures: 10 K, 290 K, 490 K, 690 K and 990 K, assuming a surface coverage of $\theta = 0.1$ (our derivation of the expression (14) for the work of formation is valid only for small coverages, and the dependence of the work of formation on the value of θ for $\theta \ll 1$ is insignificant). The formation energy and the work of formation at zero temperature differ only by the zero-point energies. The comparison of the work of formation at $T = 10$ K and the zero temperature formation energy, shown in Figs. 1 and 3(a), demonstrates that the contribution due to the zero-point vibrational energies is insignificant at this temperature as it does not change the relative positions of the curves for each cluster type. Looking at the data presented in Fig. 3, it can also be seen that raising the temperature increases the work of formation of the clusters, particularly those with larger N. At 990 K the work of

formation is increased (becomes more positive) by almost 2 eV for the largest 16 C atom cluster. An overall increase in the work of formation with temperature will naturally increase the size of the nucleation barrier and hence will also affect the critical cluster size.

For all temperatures it is noticeable that there are two size ranges where there is a nucleation barrier to overcome before the clusters can further increase in size. The first of these is in the region of $N = 4$ and 5, which occurs at a point where arching clusters become more stable than chains. The second barrier occurs for clusters sizes N between 9 and 11. In this region, first arching, then TH, and finally dome structures become more stable, and as N increases further the domes become the most favourable of all considered types. This is explained mostly by the fact that domes have fewer low-coordinated peripheral C atoms than the TH clusters. In the temperature range of 10 K - 290 K the two nucleation barriers have a similar height of around 1 eV. However as the temperature increases, the second barrier becomes larger (more positive), and therefore the barrier at 990 K will have the dominant influence on the cluster growth. Based on these results, we can conclude that once the first barrier has been overcome, clusters in the size range of C_5-C_9 will be formed but will not be able to grow further until the second barrier is overcome. More specifically this means that at high enough temperatures C_5-C_6 arching clusters may be long lived on the surface before the barrier at $N = 10$ is overcome. This means that there will be a large concentration of these clusters which may contribute directly to the graphene growth front, as suggested in[8,42] where it was reported that graphene growth proceeds by the addition of clusters of five carbon atoms. For 490-990 K an additional small barrier (≈ 0.2 eV) appears at around $N = 14$, affecting the growth of domes.

When comparing the work of formation of the various cluster types, there are similar trends as found for the zero temperature case. For clusters containing between five and nine atoms, arching clusters generally have a lower work of formation than

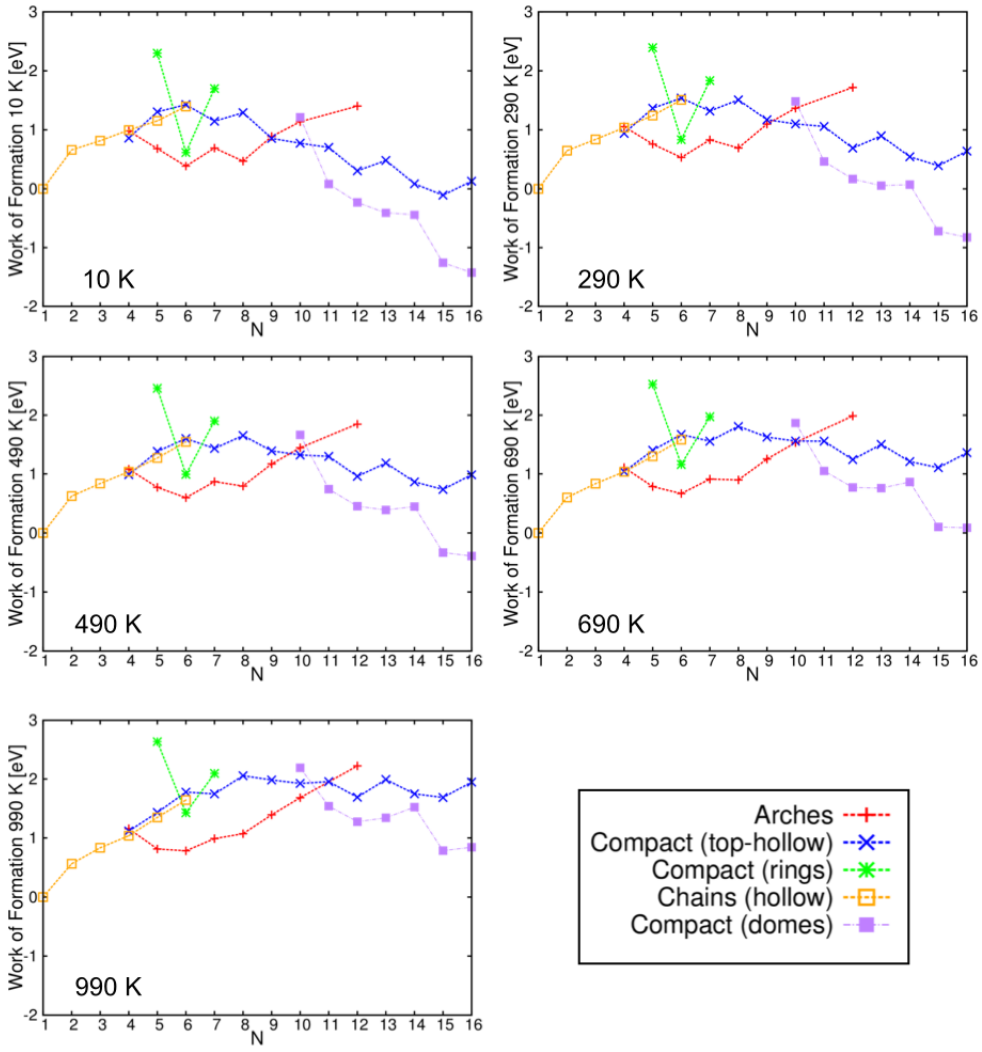

FIG. 3. The work of formation (the grand potential difference, $\Delta\phi(N)$, Eq. (14)), of various carbon clusters at different temperatures: 10 K, 290 K, 490 K, 690 K and 990 K. The work of formation is defined relative to that for the single carbon atom adsorbed on the surface.

other cluster types, the rings are less favourable than arches, and the TH clusters, even though the most stable at around $N = 10$, lose this primary position in stability at larger sizes, although becoming more favourable than arches. From $N = 11$, the domes are the most energetically favourable structures for all tem-

peratures, and therefore are likely to become the predominant cluster type during the early stages of graphene growth. These clusters have been observed during growth experiments on Ru(0001) at 900-1000 K[4] and were also shown to be very stable in previous (corresponding to zero temperature) DFT calculations[6].

The outlined trend in the calculated work of formation for arches and TH clusters is similar to the results of other studies[12,13], which have suggested that for $N = 1-10$ non-compact clusters should be more stable than compact clusters. However, since we considered additional compact cluster structures (TH and domes), we find instances where this is not the case, an example of this is found for $N = 4$ clusters. Furthermore our approach has indicated that the stability of clusters is temperature dependent.

From these results, we can make some important conclusions about the nucleation and growth of carbon clusters observed in epitaxial graphene growth. The presence of two critical cluster sizes at $N = 4 - 5$ and $N = 9 - 11$ suggests that clusters in the size range between these barriers may be metastable on the surface. Only once the second nucleation barrier is overcome will cluster growth become favourable (the smaller third barrier around $N = 14$ should be easily overcome at that stage). Increasing the temperature increases the size of the *overall* nucleation barrier; at 990 K it reaches 2 eV. This suggests that at higher temperatures cluster growth by C monomer attachment may not be likely for clusters containing fewer than 10 C atoms. Instead it is possible that smaller stable clusters, such as C_5-C_6, which are likely to be in abundance on the surface as noted above, may attach to each other to form larger clusters. At $N = 10$ there is a general transition from linear clusters being more stable to compact clusters (TH and domes) being more stable. As N increases further, dome-like clusters become the most stable. Therefore we can expect that the domes will become the predominant cluster type above $N = 12$. This is in agreement with what is observed experimentally[4]. As domes reach the size of around N =14, their further growth would proceed by attachment of either

monomers or small clusters.

C. Vibrational free energy dependence on cluster type

In Figure 3 it is noticeable that the change in the work of formation with temperature varies depending on the cluster type. For example, at $N = 12$ the energy of the dome cluster changes drastically as T increases from 10 K to 990 K, whereas the work of formation for the arch cluster increases only slightly over the same temperature range. This can be explained in terms of the vibrational frequency modes of the different cluster types. As a representative example, we show in Figure 4(a) the phonon DOS for the C_{12} arch, dome and TH clusters. Comparing the different clusters, we find that the arch structure has more low and high frequency modes than the other structures. TH clusters have fewer high and low frequency modes than either the dome and arch structures. The presence of low frequency modes will have the greatest effect on the vibrational free energy, as calculated by Eq. (10).

The temperature variation of the vibrational free energy component of the work of formation, $\Delta F^{\mathrm{vib}}(N) - N\Delta F^{\mathrm{vib}}(1)$, for each of the clusters at $N = 12$, is shown in Figure 4(b). The vibrational free energy of the C_{12} arch structure shows the greatest change with temperature, owing to its many low frequency modes. However, this negative vibrational component for the arch structure, see Figure 3, is offset by the positive coverage term in the work of formation of Eq. (10), and hence it does not change greatly with temperature. For the dome and TH clusters the vibrational free energy is either positive or negative, and we instead see a bigger change in the work of formation with temperature. This effect is greatest for the dome structure since its vibrational free energy is less negative at high temperatures, resulting in a large increase in $\Delta F(N)$. Based on these results, we can expect a similar situation for clusters with different sizes as the phonon

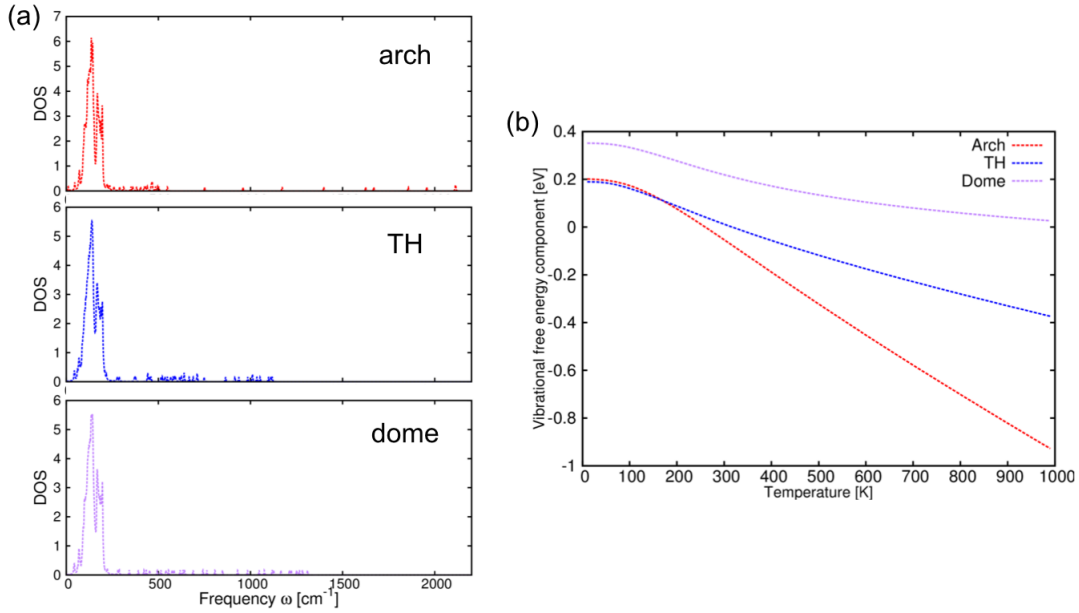

FIG. 4. (a) The phonon DOS and (b) the vibrational free energy component of the work of formation (given as $\Delta F^{\mathrm{vib}}(N) - N\Delta F^{\mathrm{vib}}(1)$) for the three different C_{12} cluster types.

DOS should depend on the cluster's structure. Domes on average have fewer low frequency modes and hence have a more positive vibrational free energy component in the work of formation. This causes their work of formation to be larger at both low and high temperatures compared to the other cluster types.

IV. CLUSTER EVOLUTION

The carbon clusters are grouped into their different types based on their structure. Because of the differences between structure types it is unlikely that clusters can reconstruct from one type to another as this would require overcoming large energy barriers related to breaking multiple bonds between C atoms and those with the surface. A cluster would be expected to grow into a larger cluster of the same type when C monomers are attached. However our results show that different cluster

types are stable over different size ranges. This suggests that less energetically stable clusters have a finite lifetime and may transform to a different cluster type which is more energetically favourable. Here we discuss energetics (in terms of DFT total energies) of such transformations for a few important cases.

As examples of such transformations, all studied using the NEB method, we first discuss two cluster reconstructions: (i) from the C_7 arch cluster to the C_8 TH cluster, and (ii) from the C_{10} TH cluster to the C_{11} dome cluster, Fig. 5. In both cases a single C atom is added. The former case, C_7(arch) + C $\rightarrow$ C_8(TH), is considered as an example of a possible early transformation from the arch to the TH family (it might be expected (see Fig. 3) that a smaller barrier would be needed for, e.g., the C_{10}(arch) + C $\rightarrow$ C_{11}(TH) transformation). At $N = 9$ the TH clusters replace the arches as the most stable type; hence it is interesting to consider how the *previous* (with $N = 8$) TH cluster can be formed after a single C atom is added to the C_7 arch. Once the C_8 TH cluster is formed, the next cluster (C_9 TH) obtained upon adding an additional C atom to it, would become the most favourable, initiating the TH type growth sequence. In the second case, in order to investigate the initiation of the dome sequence, we consider the formation of the $N = 11$ dome cluster formed by adding a single C atom to the C_{10} TH cluster. This represents the important stage during the cluster growth where the most stable cluster type changes: the considered transformation, C_{10}(TH) + C $\rightarrow$ C_{11}(dome), initiates the most favourable type sequence (the domes) from the TH type.

In the first case, Fig. 5(a), the C atom is added to the centre of the arch, and allows the inner atoms to connect to the surface and then flatten to form the compact TH structure. The energy barrier for the direct process is 1.07 eV, while the reverse barrier is 1.41 eV. Note that the C_8 TH cluster is lower in energy by almost 0.4 eV than the C_7 arch and a single C atom. Hence, by overcoming an energy barrier of just over 1 eV, the new TH sequence can indeed be initiated from

the arches even starting from $N = 7$.

In the second case of the TH-to-dome reconstruction depicted in Fig. 5(b), the C atom is added to the C_{10} TH cluster to complete a hexagonal ring. The cluster then rotates while the remaining dangling C atoms close up to form two pentagons, yielding the C_{11} dome cluster. The forward process energy barrier is around 3 eV, and the reverse process barrier is around 3.45 eV. It is seen that this transformation requires overcoming significant energy barriers, and hence may be unlikely.

Another interesting case is the C_3 chain which, according to Fig. 2, upon addition of an extra C atom may continue as the C_4 chain cluster or transform into either the C_4 arch or TH cluster. The simulated transformation processes for all three cases are shown in Fig. 6. We find that the energy barrier for forming the C_4 chain and arch is 1.8 eV, while for the C_4 TH structure the barrier is much lower, 0.96 eV. The main difference between forming the TH structure and the chain or arch structures is that the fourth C atom is added to the centre of the C_3 structure rather than at its edge. This suggests that addition of C atoms to the centre is more favourable and we should therefore expect that the continued growth of both arches and chains by monomer addition may be limited. These competitive processes are important at the onset of cluster growth since the process with the lowest energy barrier will direct the growth towards that particular cluster type. Hence, it follows from our simulations that the TH type sequence might be initiated in the early stages of clusters growth.

The calculated barriers for reconstructing the clusters from one type to another are significant especially for the TH-to-dome sequences where the barrier was found to be over 3 eV. These large barriers reflect the clusters' need to reorient themselves on the surface (which requires many bonds to break). The large barriers suggest that growth of clusters at the nucleation stage with $N > 10$ may take place by adding more than one C atom at a time. Indeed, it seems that adding three atoms from three directions to the C_{10} TH cluster would immediately form the very stable

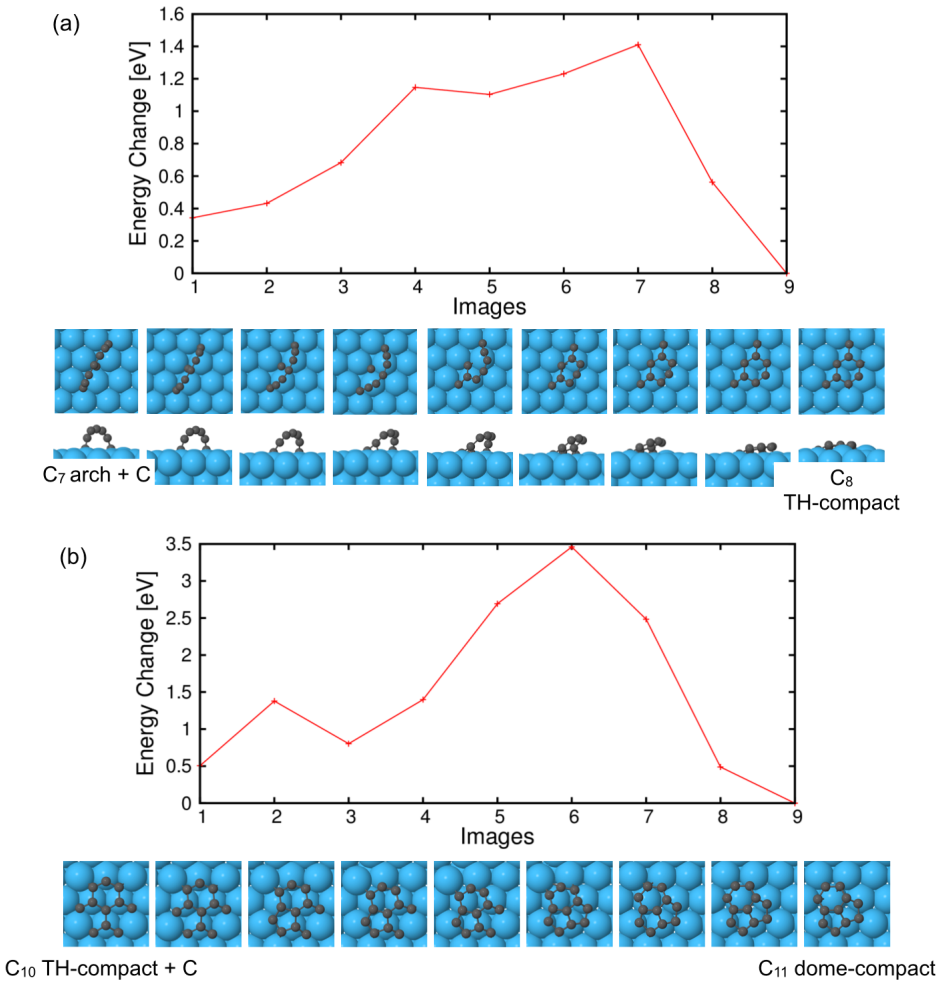

FIG. 5. The initial, intermediate and final states, along with the calculated energy profile (relative to the final state), are shown for the reconstruction of (a) the C arch cluster with an additional C atom into the C_8 TH cluster, and (b) the C_{10} TH cluster with an additional C atom into the C_{11} dome.

C_{13} dome. Another possibility is that the addition is made by small clusters as was suggested experimentally[8] and theoretically, based on rate equations[42]. Yet another possibility is that the clusters of a particular type will grow until they reach a size where they become too unstable, and then break apart. There are many possible processes whereby different clusters can grow, reconstruct and decompose,

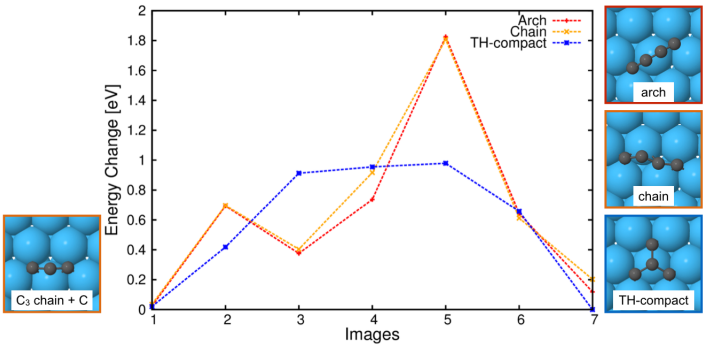

FIG. 6. The initial and final structures for the transformations of the C_3 chain into either the C_4 chain, arch or TH clusters.

which makes a complete study very difficult. However based on our results of the work of formation and the experimental and theoretical work[3,4,6], it is deduced that dome-like clusters are the dominating cluster type at the early stages of graphene growth.

As was mentioned above, based on the energy barriers for the formation of C_4 clusters from the C_3 chain, the C_4 TH cluster will likely be formed in preference to the chain and arch structures, and therefore we can expect that the TH clusters will continue to grow into larger compact clusters. This could lead to their becoming the predominant cluster type despite being less favourable compared to the arching clusters. At the same time, we cannot exclude the possibility that TH clusters with N between 5 and 9 might form arches, as the energy barrier for such a transformation may be not very significant (1.41 eV in the case of the transformation of the C_8 TH into the C_7 arch and a single C atom, see Fig. 5(a)).

V. DISCUSSION

We have presented a treatment of graphene nucleation based almost exclusively on nucleation thermodynamics which allows the statistical dynamics of the process to be studied using *ab initio* DFT based methods. To achieve this we have derived a

general expression for the work of formation of clusters of a single atomic species on a crystal surface starting from the 2D atomic gas in the low concentration limit. Temperature dependent free energy terms due to the cluster's vibrational modes and configurational entropy were included explicitly in the final formula. Using this expression, the work of formation of various carbon clusters C_N for $N = 1-16$ on the Ir(111) surface was calculated using an *ab initio* DFT method.

Our results show that the magnitude of the cluster work of formation increases with temperature; moreover, this increase becomes more noticeable for larger clusters. We find that clusters C_N of the different types considered (chains, arches, top-hollow and domes) are the most stable in various windows of N: starting from monomers, chains are replaced by arches around $N = 4$, then top-hollow clusters follow around $N = 9-10$, and finally for $N > 10$, domes with a clearly recognised hexagonal atomic arrangement become the most energetically favourable type, with a work of formation that clearly reduces every time an extra carbon atom is added to the cluster. Hence, we find for the coverage considered that linear clusters (chains and arches) are the most stable structures for N up to around 10, whereas compact structures are more stable for larger clusters. We note that the work of formation of some clusters, such as the arching clusters, have a stronger temperature dependence than others. This is due to the magnitude of their vibrational free energy.

General trends for the cluster stability obtained here broadly agree with previous zero temperature studies[12,18,29,30]. We have shown, therefore, for the first time, that the expected sequence of cluster transitions remains the same as the temperature is raised. This result is very important, , especially considering the high temperatures required for graphene growth. We have demonstrated the numerical importance of entropic terms in the free energy and that such terms should not be ignored when computing the work of formation of carbon clusters at these temperatures.

The calculated work of formation for carbon clusters has a rather peculiar form,

which is qualitatively different from the one-peak situation assumed by the standard classical nucleation theory. We find that the work of formation in our case has several maxima corresponding to a change in the type of the most stable cluster as the cluster size N increases. In particular, we are able to conclude that clusters with $N = 5 - 6$, which corresponds to a minimum in the work of formation for cluster sizes in the range of $1 \leq N < 10$, may be abundant on the surface at temperatures that are insufficient to overcome the second barrier in the work of formation. This agrees with previous experimental[8] and theoretical observations[42] that suggested that these cluster sizes may play an important role in the nucleation of graphene flakes. Once the second barrier is overcome, dome-like clusters become the most energetically favourable, with their work of formation decreasing with cluster size, hence paving the way to larger hexagonal-like structures which eventually become graphene flakes upon further growth.

There are two effects which we neglected in our study: (i) the role of anharmonicity and (ii) thermal expansion of the Ir substrate. The first effect is very difficult to calculate; it could be a matter of a separate study. Concerning the effect of the thermal expansion on the work of formation, a consistent calculation also presents a separate, quite extensive study in which the free energy of the bulk Ir is to be calculated at different temperatures and unit cell volumes, so that the equilibrium lattice constant at each T is found at the free energy minimum. Instead of performing this type of calculations, we have made an estimate of the role of the thermal expansion on the value of the quantity $\Delta F^{\rm vib}(1) = F^{\rm vib}(1) - F_0^{\rm vib}$, which corresponds to the difference of two vibrational free energies (see the paragraph preceding Eq. (12)): due to a single carbon atom adsorbed on the surface, $F^{\rm vib}(1)$, and the surface itself, $F_0^{\rm vib}$. In these calculations we used the lattice constant corresponding to 990 K (taken from Ref.[43]), which is by 1.2% larger than the value at zero temperature. We find that both free energies become more negative by a considerable amount of over 2.6 eV. At the same time, their difference, i.e.

the actual quantity of interest, $\Delta F^{\mathrm{vib}}(1)$, changed only by 0.03 eV. We believe that this is an indication that the effect of the thermal expansion on the vibrational contribution to the work of formation is very small, at least in our particular case.

The described picture is, however, only a part of the story as it corresponds to a view based exclusively on *thermodynamics,* which only provides information on the *expected* populations of different clusters at *thermodynamic equilibrium.* In order to understand the *timescale* of the nucleation process, we should consider the *kinetics* of cluster transformation from a less to a more favourable type. Intuitively, it seems that extra carbon atoms attach to clusters at their periphery, thereby keeping the same cluster type. This may result in clusters which are less thermodynamically favourable than some other cluster types of the same size. However, since cluster rearrangement would require breaking many bonds, a transformation to clusters of lower free energy is constrained by high energy barriers. Consideration of the kinetics of nucleation requires the calculation of the rates of transformation between all clusters by the addition of one, two, three, etc. carbon atoms and also possibly of various small carbon clusters. The surface mobility of all these species should be established as well. This information would enable consideration of the time evolution of clusters of different sizes and shapes (e.g. using the kinetic Monte Carlo method[44]) and hence allow us to establish the timescale for the nucleation of hexagonal flakes (large dome-like clusters).

However, such an exhaustive study of kinetics goes far beyond the present work. Instead, just to emphasise the importance of nucleation kinetics, we have only considered a few critical processes which, in our view, illustrate well the kinetics aspect of nucleation for our system. The first process corresponds to an extra carbon atom being added to a C_3 chain cluster. In this case, three almost equally stable C_4 can be formed: the arch, top-hollow or chain types. The NEB calculations indicate, however, that of all these three possibilities, the formation of a

certain top-hollow C_4 cluster has the lowest energy barrier, of under 1 eV (and hence, the highest transition rate). This seems to suggest that it is most likely that once the C_3 chain clusters are formed, many of them would transform into the C_4 top-hollow cluster initiating the growth of these types of compact clusters. The latter clusters, however, are not the most favourable until about $N = 9 - 10$, so it is also possible that the smaller top-hollow clusters may transform into the arch cluster type which is the most favourable. However, after about $N = 9$ the top-hollow clusters become more stable. Hence, we considered a process of adding an extra C atom to a C_7 arch in order to calculate the energy barrier for transforming it into the C_8 top-hollow cluster, and found that this energy barrier (just over 1 eV) is not significant for the temperatures at which the graphene is grown. Once the C_8 top-hollow cluster is formed, adding an extra carbon atom to it leads to the C_9 cluster, hence initiating this type sequence.

However, the next process we have considered, the transformation of the C_{10} top-hollow (with one extra C atom) into the C_{11} dome-like cluster, indicated a complex picture of cluster growth. Indeed, according to our calculations of the work of formation, if the C_{11} domes were formed, further additions of C atoms would result in even more stable clusters, thereby initiating the formation of the dome sequence. At the same time, the calculated energy barrier for the required initial transformation process, $C_{10}(\mathrm{TH}) + \mathrm{C} \rightarrow C_{11}(\mathrm{dome})$, was found to be too large (over 3 eV) which seems to suggest that the switch from the top-hollow to dome type happens in a different way. Since we have established that C_5-C_6 clusters are expected to be present in large quantities on the surface during cluster growth, we speculate that these clusters play an essential role in initiating the dome sequence, in contrast to the addition of carbon atoms individually to the top-hollow clusters.

VI. CONCLUSIONS

In this paper we derived, using a statistical-mechanical argument, an expression for the work of formation of carbon clusters adsorbed on the Ir(111) surface as a function of their size and temperature. The DFT based calculations revealed a complex character of the work of formation, which demonstrates several maxima as a function of the cluster size N. Alongside thermodynamic aspects, essentially based on ideas of classical nucleation theory, kinetics aspects of the cluster's nucleation were also discussed. It is clear that more studies are needed to establish the detailed mechanism of carbon clusters growth and hence to understand the process of graphene nucleation. We hope that this study will stimulate further research in the directions indicated.

VII. SUPPLEMENTARY MATERIAL

See the supplementary material for the zero temperature formation energies of additional clusters.

VIII. ACKNOWLEDGEMENT

Through our membership of the UK's HPC Materials Chemistry Consortium, which is funded by EPSRC (grants EP/F067496, EP/L000202), this work made use of the facilities of HECTOR and ARCHER, the UK's national high-performance computing service, which is funded by the Office of Science and Technology through EPSRC's High End Computing Programme.

REFERENCES

[1]H. Tetlow, J. Posthuma de Boer, I. J. Ford, D. D. Vvedensky, J. Coraux, and L. Kantorovich. *Phys. Rep.* **542**, 195 (2014).

[2]J. Coraux, A. T. N'Diaye, M. Engler, C. Busse, D. Wall, N. Buckanie, F.-J. Meyer zu Heringdorf, R. van Gastel, B. Poelsema, and T. Michely. *New J. Phys.* **11**, 023006 (2009).

[3]B. Wang, X. Ma, M. Caffio, R. Schaub, and W.-X. Li. *Nano Lett.* **11**, 424 (2011).

[4]Y. Cui, Q. Fu, H. Zhang, and X. Bao. *Chem. Commun.* **47**, 1470 (2011).

[5]H. Tetlow, J. Posthuma de Boer, I. J. Ford, D. D. Vvedensky, D. Curcio, L. Omiciuolo, S. Lizzit, A. Baraldi, and L. Kantorovich. *Phys. Chem. Chem. Phys.* **18**, 27897 (2016).

[6]P. Lacovig, M. Pozzo, D. Alfè, P. Vilmercati, Al. Baraldi, and S. Lizzit. *Phys. Rev. Lett.* **103**, 166101 (2009).

[7]J. Gao and F. Ding. *J. Phys. Chem. C* **119**, 11086 (2015).

[8]E. Loginova, N. C. Bartelt, P. J. Feibelman, and K. F. McCarty. *New J. Phys.*. **10**, 093026 (2008).

[9]S. Chandrasekhar. *Rev. Mod. Phys.* **15**, 1 (1943).

[10]I. J. Ford. *Proc. Instn Mech. Engnrs Part C: J. Mech. Eng. Sci.* **218**, 883 (2004).

[11]V. I. Kalikmanov. *Nucleation Theory.* Springer, 2012.

[12]P. Wu, H. Jiang, W. Zhang, Z. Li, Z. Hou, and J. Yang. *J. Am. Chem. Soc.* **134**, 6045 (2012).

[13]C. Herbig, E. H. Åhlgren, W. Jolie, C. Busse, J. Kotakoski, A. V. Krasheninnikov, and T. Michely. *ACS Nano.* **8**, 12208 (2014).

[14]R. G. Van Wesep, H. Chen, W. Zhu, and Z. Zhang. *J. Chem. Phys.* **134**, 171105 (2011).

[15]J. Gao and J. Zhao. *Eur. Phys. J. D* **67**, 1 (2013).

[16]P. Wu, W. Zhang, Z. Li, and J. Yang. *Small.* **10**, 2136 (2014).

[17]E. C. Neyts, Y. Shibuta, A. C. T. van Duin, and A. Bogaerts. *ACS Nano.* **4**, 6665 (2010).

[18]A. J. Page, I. Mitchell, H.-B. Li, Y. Wang, M.-G. Jiao, S. Irle, and K. Morokuma. *J. Phys. Chem. C* **120**, 13851 (2016).

[19]Q. Yuan, J. Gao, H. Shu, J. Zhao, X. Chen, and F. Ding. *J. Am. Chem. Soc.* **134**, 2970 (2012).

[20]J. Gao, J. Yip, J. Zhao, B. I. Yakobson, and F. Ding. *J. Am. Chem. Soc.* **133**, 5009 (2011).

[21]D. Cheng, G. Barcaro, J.-C. Charlier, M. Hou, and A. Fortunelli. *J. Phys. Chem. C* **115**, 10537 (2011).

[22]G. Barcaro, B. Zhu, M. Hou, and A. Fortunelli. *Comp. Mat. Sci.* **63**, 303 (2012).

[23]Z. Xu, T. Yan, G. Liu, G. Qiao, and F. Ding. *Nanoscale.* **8**, 921 (2016).

[24]Y. Ohta, Y. Okamoto, A. J. Page, St. Irle, and K. Morokuma. *ACS Nano.* **3**, 3413 (2009).

[25]E. C. Neyts and A. C. T. van Duin adn A. Bogaerts. *Nanoscale.* **5**, 7250 (2013).

[26]J. Y. Raty, F. Gygi, and G. Galli. *Phys. Rev. Lett.* **95**, 096103 (2005).

[27]M. Moors, H. Amara, T. Visart de Bocarm, C. Bichara, F. Ducastelle, N. Kruse, and J.-C. Charlier. *ACS Nano.* **3**, 511 (2009).

[28]H. Amara, C. Bichara, and F. Ducastelle. *Phys. Rev. Lett.* **100**, 056105 (2008).

[29]C.-M. Seah, S.-P. Chai, and A. R. Mohamed. *Carbon.* **70**, 1 (2014).

[30]A. J. Page, F. Ding, S. Irle, and K. Morokuma. *Rep. Prog. Phys.* **78**, 036501 (2015).

[31]J. A. Elliot, Y. Shibuta, H. Amara, C. Bichara, and E. C. Neyts. *Nanoscale.* **5**, 6662 (2013).

[32]I. J. Ford. *Phys. Rev. E.* **56**, 5615 (1997).

[33]J. Hutter, M. Iannuzzi, F. Schiffmann, and J. VandeVondele. *Wiley Interdiscipl. Reviews: Comp. Mol. Sci.* **4**, 15 (2014).

[34]J.P. Perdew, K. Burke, and M. Ernzerhof. *Phys. Rev. Lett.* **77**, 3865 (1996).

[35]S. Goedecker, M. Teter, and J. Hutter. *Phys. Rev. B* **54**, 1703 (Jul 1996).

[36]J. VandeVondele and J. Hutter. *J. Chem. Phys.* **127**, 114105 (2007).

[37]S. Grimme, J. Antony, S. Ehrlich, and H. Krieg. *J. Chem. Phys.* **132**, 154104 (2010).

[38]H. Jonsson, G. Mills, and K. W. Jacobsen. *Classical and Quantum Dynamics in Condensed Phase Simulations*, chapter Nudged Elastic Band Method for Finding Minimum Energy Paths of Transitions. World Scientific, 1998.

[39]G. Mills, H. Jonsson, and G. K. Schenter. *Surf. Sci.* **324**, 305 (1995).

[40]G. Henkelman and H. Jónsson. *J. Chem. Phys.* **113**, 9978 (2000).

[41]G. Henkelman, B. P. Uberuaga, and H. Jónsson. *J. Chem. Phys.* **113**, 9901 (2000).

[42]J. Posthuma de Boer, I. J. Ford, L. Kantorovich, and D. D. Vvedensky. *J. Phys.: Condens. Matter*. **26**, 185008 (2014).

[43]J. W. Arblaster. *Platinum Metals Rev.* **54**, 93 (2010).

[44]K. A. Fichthorn and W. H. Weinberg. *J. Chem. Phys.* **95**, 1090 (1991).